May, 1993] Bull. Chem. Soc. Jpn., 66, 1501—1510(1993)

X-Ray Structural Investigation of the Chiral Recognition of Brucine in Salt Formation with an N-Protected Amino Acid, *N*-Phthaloyl-*threo*-β-hydroxy-D- and L-leucine

Shigeru KUWATA, Jumpei TANAKA, Norihiro ONDA, Takashi YAMADA, Toshifumi MIYAZAWA,
Makiko SUGIURA,† Yasuko IN,†† Mitsunobu DOI,†† Masatoshi INOUE,†† and Toshimasa ISHIDA*,††
Department of Chemistry, Faculty of Science, Konan University, 8-9-1 Okamoto, Higashinada-ku, Kobe 658
† Kobe Women's College of Pharmacy, 4-19-1 Motoyamakita-machi, Higashinada-ku, Kobe 658
†† Osaka University of Pharmaceutical Sciences, 2-10-65 Kawai, Matsubara, Osaka 580

(Received December 17, 1992)

In order to determine how brucine recognizes the chirality of an N-protected amino acid in complex formation, three kinds of brucine complex crystals of *N*-phthaloyl-*threo*-β-hydroxyleucines, i.e., two (yellow and transparent) crystals for the L-isomer and one (transparent) crystal for the D-isomer, were prepared, and their structures were determined by X-ray crystallography. In addition to the interaction mode specific for each complex crystal, the carboxyl and β-hydroxyl groups of the amino acids were commonly linked with the methoxyindole and piperidine ring moieties of brucine through hydrogen bonds and electrostatic and van der Waals interactions. In addition to the direct interactions between the molecules, the molecular arrangement of brucine in the crystal structure played an important role in the D/L-recognition of the amino acids. The molecular packing of the brucine molecules translated by a crystallographic 2-fold screw symmetry operation provided a shape for the cavity that was most suitable for binding with the D-isomer. In contrast, two crystallographically independent brucine molecules participated in recognizing the L-isomer, where the arrangement of these molecules in the crystal structure formed a receptor surface suitable for binding with the L-isomer. In this paper, an explanation of how brucine recognizes the D/L-isomer in the crystalline state is presented.

Brucine (**1** in Fig. 1), an indole alkaloid isolated from the seeds of *Strychnos nuxvomica* and related plants, has been widely used as a resolving agent for racemic mixtures of N-protected chiral amino acids. In a large number of cases, it was found that one of the diastereometric salts was very much less soluble than the other, and preferentially crystallized out of the solution.

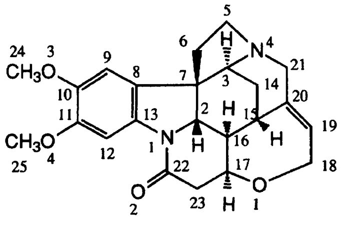

1

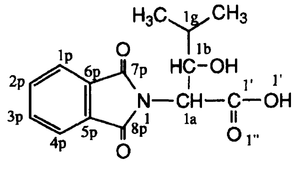

2

Fig. 1. Chemical structures of brucine (**1**) and phthaloyl-*threo*-β-hydroxyleucine (**2**), and their atomic numberings used in this work.

Despite many successful resolutions of racemates by this technique,[1] however, there is very little explanation or rationalization[2] concerning the resolving mechanism at the atomic level. All the crystal structures of the brucine–amino acid and related complexes so far analyzed[2,3] are restricted to either one of the D/L diastereomeric pairs and there are no reports concerning the comparative investigation of the crystal structures of both diastereomers, although this would provide a molecular basis for understanding how brucine molecules recognize the chiral center of an amino acid.

In attempting the optical resolution of the *threo*-β-hydroxyleucine recemate, the L-form of which is needed to synthesize leucinostatin C or D,[4] a novel peptide antibiotic from *Paecilomyces fungi*, three kinds of crystals were obtained in the complex preparation of its *N*-phthaloylated recemate (Pht-threo-Hyleu) (**2**) with brucine, according to the scheme shown in Fig. 2.[5] When the brucine mixture of the **2** racemate was crystallized from ethanol, crystals of Complex I (D-isomer) and Complex II (L-isomer) were obtained in whitish and yellow colors, respectively. Thus, this color difference leads to optical separation by mechanical means.[5] The present paper deals with the crystal structures of Complexes I, II, and III (L-isomer). The comparison of these complexes is important to understand how brucine recognizes the D/L-isomers of **2**. In this paper, brucine and *N*-phthaloyl-*threo*-β-hydroxyluecine molecules are abbreviated as BC and PL, respectively.

Experimental

Syntheses and Crystallization. According to

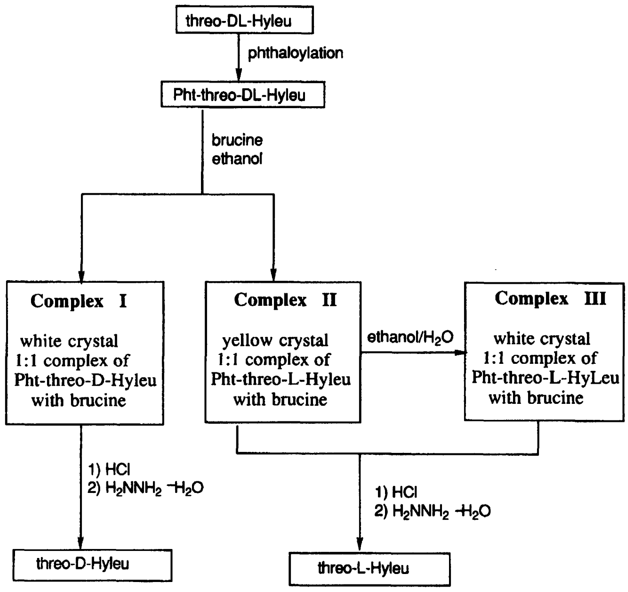

Fig. 2. Optical resolution scheme for *threo*-β-hydroxylecine racemates.

Kuwata et al.,$^{5)}$ the PL racemate was synthesized from isobutyraldehyde, glycine, and phthalic anhydride. As shown in Fig. 2, crystals of BC complexed with PL D-isomer (Complex I) and L-isomer (Complexes II and III) were prepared and used for the subsequent X-ray study; Complex II was recrystallized from a methanol solution because of the good crystallinity compared with that from ethanol. The coexistence of solvent molecules was checked by NMR measurements.

Crystal Data and Intensity Collection. Details of the crystallographic data and parameters or conditions for the X-ray reflectional intensity collections are summarized in Table 1. Unit-cell dimensions were determined by a least-squares fit of 2θ angles for 25 reflections of $30° < 2\theta < 60°$, which were measured by graphite-monochromated Cu $K\alpha$ radiation ($\lambda = 1.5418$ Å) on an automated Rigaku AFC-5 diffractometer. Intensity data were collected with the same diffractometer, where the background was counted for 5 s at both extremes of each peak. Four standard reflections were monitored for every 100 reflection intervals and showed no significant time dependence ($< \pm 2\%$). The observed intensities were corrected for Lorentz and polarization effects. No corrections for absorption or extinction effects were made for crystals.

Crystal Structure Solution and Refinement. The crystal structures of Complexes I and III were solved by the direct method by using the SHELXS86 program.$^{6)}$ The structure of Complex II was solved by a vector search procedure in the PATSEE computer program$^{7)}$ using the atomic coordinates of the BC–PL pair in Complex III.

Full-matrix, anisotropic least-squares refinements were performed on non-H atoms using the SHELX-76 program.$^{8)}$ Ideal positions of H atoms were calculated and included in subsequent refinements with isotropic thermal factors; the existence of these H atoms was also verified on a difference Fourier map. The least-squares refinements were executed in alternating blocks, each block consisting of the coordinates and thermal parameters for a BC or PL molecule. Although solvent molecules in Complexes II and III were found at the full occupancies, the oxygen atom of ethanol in Complex I was disordered into two positions with one-half occupancy.

The function minimized was $\sum w(|F_o| - |F_c|)^2$, and the weighting scheme used for the refinement was $w = 1.0/[\sigma(F_o)^2]$. Final R, R_w, and S are given in Table 1. None of the positional parameters for non-H atoms shifted more than their esds, and the residual electron densities in the final difference Fourier map were all in the range of -0.29—0.35 e Å^{-3}. Fractional coordinates and isotropic temperature factors for non-H atoms are given in Tables 2, 3, and 4.$^{9)}$

All numerical calculations were performed on a MicroVAX II computer at the Computation Center, Osaka University of Pharmaceutical Sciences.

Results and Discussion

Crystal Structure. Stereoscopic views of the respective crystal structures are shown in Fig. 3, where PL molecules are shaded and solvents are depicted with filled circles. The crystal structures of Complexes II and III contained two crystallographically independent BC and PL molecules (two complex pairs) per asymmetric unit, and they were classified as molecules A and B for BC and PL, respectively.

The crystal structure of Complex I conserves the characteristics of brucine molecular packing most commonly observed in complex crystals with guest molecules,$^{2)}$ i.e., the brucine molecules compose corrugated monolayer sheets which are oriented perpendicularly to the longest crystal axis ($= b$), and these sheets are separated by channels containing the guest and solvent molecules. This separation distance is dependent on the molecular size of the guest molecule and is ca. 13.6 Å ($= b/2$) for the PL molecule. Although such characteristic packing of brucine could be traced, the crystal structures of Complexes II and III give rather different packing diagrams. In the crystal structure of Complex II, both BC and PL molecules form infinite and corrugated monolayer sheets along the c-direction, in which the phthaloyl moieties of PL are partially overlapped with BC molecules. The translation of these sheets by a crystallographic 2-fold screw symmetry along the a-axis makes double-layered pillers with a width of ca. 7.7 Å ($= b/2$) and a depth of ca. 14.1 Å ($= a/2$). In the crystal structure of Complex III, two independent BC molecules pile up alternately along the c-direction and form infinite stacking layers. The PL and solvent molecules are sandwiched between these layers.

Solvent molecules are located at the cavities created by the crystal packing of both molecules and stabilize the complex structure by hydrogen bonds and/or van der Waals contacts with neighboring polar atoms (Table 5). It is interesting to note that each of two water molecules in Complex III forms two hydrogen bonds with neighboring carboxyl oxygen atoms, thus tightening the molecular arrangement of two independent PL molecules.

Table 1. Cell Parameters and Details of Intensity Data Collection and Structure Analyses

	Complex I D-isomer	Complex II L-isomer	Complex III L-isomer
Color	Transparent	Yellow	Transparent
Formula	$C_{14}H_{14}NO_5 \cdot C_{23}H_{27}N_2O_4 \cdot C_2H_5OH$	$C_{14}H_{14}NO_5 \cdot C_{23}H_{27}N_2O_4 \cdot CH_3OH$	$C_{14}H_{14}NO_5 \cdot C_{23}H_{27}N_2O_4 \cdot 2H_2O$
M_r	717.81	1375.53	1379.52
Crystal system	Orthorhombic	Orthorhombic	Monoclinic
Space group	$P2_12_12_1$	$P2_12_12_1$	$P2_1$
Cell constant			
a/Å	14.494(2)	28.115(5)	16.135(2)
b/Å	27.235(4)	15.420(5)	27.099(4)
c/Å	9.118(2)	16.421(5)	7.750(1)
β/°	90	90	94.55(2)
V/Å^3	3599.3(9)	7118.9(32)	3377.8(8)
Z	4	8	4
D_c/g cm^{-3}	1.325	1.283	1.356
μ (Cu $K\alpha$)/cm^{-1}	7.00	7.26	7.78
F (000)	1528	2920	1464
Size/mm	0.5×0.3×0.2	0.5×0.2×0.1	0.5×0.2×0.2
Temp/°C	15	15	15
Scan mode	ω–2θ	ω–2θ	ω–2θ
Scan width/°	0.90+0.15 tan θ	1.40+0.15 tan θ	1.50+0.15 tan θ
Scan speed/° min^{-1}	5	5	5
2θ ragne/°	$2 \leq 2\theta \leq 130$	$2 \leq 2\theta \leq 130$	$2 \leq 2\theta \leq 130$
No. of measured reflections	3226	6660	5887
No. of used reflections	2944 ($F_o > 0.0$)	6229 ($F_o > \sigma(F_o)$)	5646 ($F_o > 0.0$)
No. of variables	666	1230	1230
R	0.059	0.066	0.051
R_w	0.068	0.088	0.069
S	1.198	0.925	0.868

A notable characteristic of these crystals is the different coloration, i.e., transparent for Complexes I and III and yellow for Complex II. The formation of continuous double-layered pillers, in which the BC and PL molecules are partially overlapped with each other, could be responsible for the yellow coloration of Complex II.

Molecular Structure and Intermolecular Interaction. The interaction modes of BC with PL molecules are shown in Fig. 4, where the interaction modes of PL molecules with the BC molecule B in Complexes II and III were omitted because they are almost the same as molecule A. Some selected torsion angles are listed in Table 6.

The bond lengths and angles of each molecule have esds of 0.005 Å (Complex III)—0.02 Å (II) and 0.2° (II and III)—0.8° (II), respectively. The esds for the disordered ethanol in Complex I were lager (0.02 Å and 0.8°—1°) because of its high thermal motion. Although the accuracy for these bonding parameters is not as high as usual, no notable abnormality was observed, and the difference among the same bond lengths and angles of BC and PL molecules appears to be in the acceptable region.

The molecular geometries of the BC molecules were all very similar. A major, but not significant, divergence was observed at the torsion angles about the six-membered ring consisting of the N(1), C(2), C(16), C(17), C(23), and C(22) atoms. They varied by 6—12° to one another concerning the same torsion angles. A similar characteristic has also been noted in the crystal structures of strychinine and BC molecules.[10] BC molecules in all the complex crystals were in a cationic form protonated at the N(4) atom; the N–C bond length, 1.489 Å—1.556 Å, was in the normal single bond distance.

The PL molecules in all the crystals had a similar conformation, and the torsion angles about respective bonds (Table 6) were all in the same region, except for the mirror image of the D/L configuration concerning the chiral C(1a) atom and for the Leu side chain. This implies that the molecular conformation of each PL molecule is little influenced by different molecular packing environments. All of the PL molecules were in an anionic form with the carboxyl terminal deprotonated; the C–O bond length, 1.217—1.261 Å, was in the anionic distance range.

Short-contact atomic pairs less than 3.5 Å are summarized in Table 5. It is noteworthy that each of two independent complex pairs in Complexes II and III essentially showed the same interaction mode to each other.

Table 2. Final Atomic Coordinates of Complex I and Equivalent Values of the Isotropic Temperature Factors with Their esds in Parentheses

Atom	x	y	z	$U_{eq}{}^{a)}/\text{Å}^2$
Brucine				
N(1)	0.4665(3)	0.9913(2)	0.8062(5)	0.051(2)
C(2)	0.4761(3)	0.9508(2)	0.6998(5)	0.042(2)
C(3)	0.6098(3)	0.8871(2)	0.6740(6)	0.050(2)
N(4)	0.5573(3)	0.8419(1)	0.6207(5)	0.057(2)
C(5)	0.4721(4)	0.8374(2)	0.7109(8)	0.068(3)
C(6)	0.4894(4)	0.8693(2)	0.8411(7)	0.056(3)
C(7)	0.5408(3)	0.9137(2)	0.7783(5)	0.043(2)
C(8)	0.5859(3)	0.9439(1)	0.8982(5)	0.041(2)
C(9)	0.6575(3)	0.9341(2)	0.9906(5)	0.047(2)
C(10)	0.6804(3)	0.9665(2)	1.0998(6)	0.050(2)
C(11)	0.6294(3)	1.0103(2)	1.1170(6)	0.050(2)
C(12)	0.5560(4)	1.0210(2)	1.0254(6)	0.054(3)
C(13)	0.5350(3)	0.9879(2)	0.9149(5)	0.047(2)
C(14)	0.6446(3)	0.9175(2)	0.5478(6)	0.055(3)
C(15)	0.5606(4)	0.9355(2)	0.4597(6)	0.060(3)
C(16)	0.5122(3)	0.9734(2)	0.5571(6)	0.049(2)
C(17)	0.4333(4)	1.0030(2)	0.4898(7)	0.059(3)
C(18)	0.3818(5)	0.9466(2)	0.3073(8)	0.086(4)
C(19)	0.4243(5)	0.8980(2)	0.3455(8)	0.075(4)
C(20)	0.5004(5)	0.8922(2)	0.4170(6)	0.066(3)
C(21)	0.5373(4)	0.8432(2)	0.4584(7)	0.069(3)
C(22)	0.4282(4)	1.0346(2)	0.7625(7)	0.064(3)
C(23)	0.3877(6)	1.0349(2)	0.6091(8)	0.084(4)
C(24)	0.8029(4)	0.9179(2)	1.1970(8)	0.073(3)
C(25)	0.6125(5)	1.0868(2)	1.2424(7)	0.072(3)
O(1)	0.3594(3)	0.9745(1)	0.4321(5)	0.068(2)
O(2)	0.4250(4)	1.0708(1)	0.8384(6)	0.089(3)
O(3)	0.7508(3)	0.9619(1)	1.1998(5)	0.066(2)
O(4)	0.6552(3)	1.0401(1)	1.2301(4)	0.065(2)
Pht-*threo*-D-Hyleu				
C(1p)	0.7218(4)	0.6019(2)	1.2026(6)	0.059(3)
C(2p)	0.6974(5)	0.5999(2)	1.3514(7)	0.074(4)
C(3p)	0.6815(5)	0.6419(2)	1.4346(7)	0.077(4)
C(4p)	0.6862(4)	0.6886(2)	1.3690(6)	0.062(3)
C(5p)	0.7102(3)	0.6903(2)	1.2212(6)	0.049(3)
C(6p)	0.7272(3)	0.6483(2)	1.1405(6)	0.046(2)
C(7p)	0.7509(3)	0.6634(2)	0.9906(6)	0.044(2)
O(7p)	0.7700(3)	0.6385(1)	0.8867(4)	0.064(2)
C(8p)	0.7234(3)	0.7330(2)	1.1230(5)	0.044(2)
O(8p)	0.7141(3)	0.7763(1)	1.1573(4)	0.058(2)
N(1)	0.7492(3)	0.7150(1)	0.9889(4)	0.042(2)
C(1a)	0.7682(3)	0.7419(2)	0.8525(5)	0.041(2)
C(1′)	0.6789(3)	0.7592(2)	0.7755(6)	0.046(3)
O(1′)	0.6057(2)	0.7593(1)	0.8408(5)	0.069(2)
O(1″)	0.6915(3)	0.7744(1)	0.6465(4)	0.057(2)
C(1b)	0.8342(3)	0.7860(2)	0.8717(6)	0.043(2)
O(1b)	0.7863(2)	0.8276(1)	0.9327(4)	0.049(2)
C(1g)	0.9229(3)	0.7744(2)	0.9533(6)	0.048(3)
C(1d1)	0.9746(3)	0.7329(2)	0.8758(7)	0.059(3)
C(1d2)	0.9837(4)	0.8190(2)	0.9637(7)	0.063(3)
Solvate				
C(1et)	0.8640(5)	0.7528(3)	1.499(1)	0.087(4)
C(2et)	0.891(1)	0.7992(5)	1.424(2)	0.17(1)
O(1et)	0.824(1)	0.8257(4)	1.475(2)	0.17(1)
O(2et)	0.9689(9)	0.8109(6)	1.421(2)	0.14(1)

a) $U_{eq}=1/3\sum_i\sum_j U_{ij}a_i^*a_j^*\mathbf{a}_i\cdot\mathbf{a}_j$.

Table 3. Final Atomic Coordinates of Complex II and Equivalent Values of the Isotropic Temperature Factors with Their esds in Parentheses

Atom	x	y	z	$U_{eq}/\text{Å}^2$
Pair I				
Brucine				
N(1)	0.6867(1)	1.0939(2)	0.1654(2)	0.044(2)
C(2)	0.7119(2)	1.0092(3)	0.1733(3)	0.036(2)
C(3)	0.6820(1)	0.8538(3)	0.1329(3)	0.036(2)
N(4)	0.7300(1)	0.8091(2)	0.1113(2)	0.042(2)
C(5)	0.7584(2)	0.8708(3)	0.0581(3)	0.049(2)
C(6)	0.7229(2)	0.9403(3)	0.0333(3)	0.046(2)
C(7)	0.6899(2)	0.9495(3)	0.1061(3)	0.039(2)
C(8)	0.6447(2)	1.0001(3)	0.0845(3)	0.041(2)
C(9)	0.6074(2)	0.9682(3)	0.0334(3)	0.056(3)
C(10)	0.5719(2)	1.0290(5)	0.0149(4)	0.075(4)
C(11)	0.5755(3)	1.1153(4)	0.0404(5)	0.076(4)
C(12)	0.6130(2)	1.1428(4)	0.0888(4)	0.066(3)
C(13)	0.6463(2)	1.0823(4)	0.1108(4)	0.055(3)
C(14)	0.6708(2)	0.8397(3)	0.2223(3)	0.041(2)
C(15)	0.7104(2)	0.8831(3)	0.2731(3)	0.040(2)
C(16)	0.7042(2)	0.9805(3)	0.2619(3)	0.041(2)
C(17)	0.7330(2)	1.0425(3)	0.3152(3)	0.049(3)
C(18)	0.7997(3)	0.9464(4)	0.3439(4)	0.068(3)
C(19)	0.7991(2)	0.8769(3)	0.2792(4)	0.056(3)
C(20)	0.7586(2)	0.8483(3)	0.2485(3)	0.045(2)
C(21)	0.7576(2)	0.7805(3)	0.1841(3)	0.045(2)
C(22)	0.6895(2)	1.1557(3)	0.2230(3)	0.056(3)
C(23)	0.7271(3)	1.1385(4)	0.2891(4)	0.069(3)
C(24)	0.5284(3)	0.9252(6)	−0.0571(6)	0.098(5)
C(25)	0.5436(6)	1.2562(6)	0.029(1)	0.19(1)
O(1)	0.7835(2)	1.0287(2)	0.3120(2)	0.058(2)
O(2)	0.6684(2)	1.2236(2)	0.2225(3)	0.077(3)
O(3)	0.5337(2)	1.0100(3)	−0.0344(4)	0.090(3)
O(4)	0.5389(2)	1.1669(4)	0.0161(6)	0.132(5)
Pht-*threo*-L-Hyleu				
C(1p)	0.5656(2)	0.5530(7)	0.3651(5)	0.111(5)
C(2p)	0.5656(3)	0.4834(8)	0.4180(5)	0.119(5)
C(3p)	0.5819(4)	0.404(1)	0.3901(7)	0.143(8)
C(4p)	0.5984(3)	0.3902(7)	0.3111(5)	0.129(6)
C(5p)	0.5959(2)	0.4555(4)	0.2597(4)	0.072(4)
C(6p)	0.5806(2)	0.5376(4)	0.2852(4)	0.069(3)
C(7p)	0.5838(2)	0.5996(4)	0.2145(5)	0.077(4)
O(7p)	0.5749(2)	0.6752(3)	0.2144(3)	0.105(4)
C(8p)	0.6096(2)	0.4626(4)	0.1726(4)	0.069(3)
O(8p)	0.6252(2)	0.4107(3)	0.1267(3)	0.089(3)
N(1)	0.5998(2)	0.5541(3)	0.1509(3)	0.063(3)
C(1a)	0.6208(2)	0.5907(4)	0.0774(3)	0.066(3)
C(1′)	0.6698(2)	0.6320(3)	0.0982(3)	0.053(3)
O(1′)	0.6865(1)	0.6196(2)	0.1660(2)	0.069(2)
O(1″)	0.6892(1)	0.6726(2)	0.0403(2)	0.056(2)
C(1b)	0.5888(3)	0.6451(5)	0.0261(5)	0.097(5)
O(1b)	0.5852(2)	0.7297(3)	0.0601(4)	0.109(4)
C(1g)	0.5387(3)	0.6066(7)	0.0081(7)	0.144(8)
C(1d1)	0.5069(5)	0.6676(8)	−0.040(1)	0.23(1)
C(1d2)	0.5473(5)	0.5179(9)	−0.0223(8)	0.19(1)

Table 3. (Continued)

Atom	x	y	z	$U_{eq}/Å^2$
Pair II				
Brucine				
N(1)	0.7953(1)	0.5794(2)	−0.0004(2)	0.043(2)
C(2)	0.7738(2)	0.4950(3)	−0.0212(3)	0.039(2)
C(3)	0.8032(2)	0.3384(3)	0.0149(3)	0.038(2)
N(4)	0.7555(1)	0.2899(2)	0.0266(2)	0.039(2)
C(5)	0.7230(2)	0.3481(3)	0.0765(3)	0.050(3)
C(6)	0.7557(2)	0.4140(3)	0.1127(3)	0.045(2)
C(7)	0.7935(2)	0.4307(3)	0.0451(2)	0.035(2)
C(8)	0.8363(2)	0.4794(3)	0.0767(3)	0.038(2)
C(9)	0.8732(2)	0.4520(3)	0.1269(3)	0.043(2)
C(10)	0.9063(2)	0.5134(3)	0.1557(3)	0.050(3)
C(11)	0.9008(2)	0.5981(3)	0.1380(3)	0.050(3)
C(12)	0.8633(2)	0.6285(3)	0.0871(3)	0.051(3)
C(13)	0.8323(2)	0.5655(3)	0.0570(3)	0.044(3)
C(14)	0.8200(2)	0.3313(3)	−0.0713(3)	0.045(3)
C(15)	0.7846(2)	0.3756(3)	−0.1278(3)	0.047(3)
C(16)	0.7883(2)	0.4751(3)	−0.1080(3)	0.044(2)
C(17)	0.7639(2)	0.5359(3)	−0.1650(3)	0.057(3)
C(18)	0.7006(2)	0.4421(4)	−0.2120(4)	0.079(4)
C(19)	0.6976(2)	0.3682(3)	−0.1539(4)	0.073(4)
C(20)	0.7355(2)	0.3390(3)	−0.1144(3)	0.049(3)
C(21)	0.7326(2)	0.2645(3)	−0.0540(3)	0.044(2)
C(22)	0.7932(2)	0.6470(3)	−0.0556(3)	0.058(3)
C(23)	0.7656(2)	0.6318(3)	−0.1302(4)	0.071(4)
C(24)	0.9591(2)	0.4022(5)	0.1984(5)	0.101(5)
C(25)	0.9238(3)	0.7413(4)	0.1695(7)	0.143(8)
O(1)	0.7117(2)	0.5213(2)	−0.1705(3)	0.084(3)
O(2)	0.8133(2)	0.7150(2)	−0.0430(3)	0.080(3)
O(3)	0.9444(1)	0.4898(2)	0.2015(3)	0.073(3)
O(4)	0.9331(1)	0.6535(2)	0.1727(3)	0.072(2)
Pht-*threo*-L-Hyleu				
C(1p)	0.9418(3)	0.037(1)	−0.1912(6)	0.156(9)
C(2p)	0.9488(3)	−0.0340(9)	−0.2401(6)	0.142(8)
C(3p)	0.9316(6)	−0.1211(9)	−0.2095(9)	0.19(1)
C(4p)	0.9105(5)	−0.1325(7)	−0.1328(7)	0.159(9)
C(5p)	0.9066(3)	−0.0592(6)	−0.0847(5)	0.104(6)
C(6p)	0.9214(2)	0.0206(6)	−0.1153(4)	0.084(5)
C(7p)	0.9088(2)	0.0890(5)	−0.0466(5)	0.084(5)
O(7p)	0.9184(2)	0.1617(4)	−0.0484(3)	0.099(4)
C(8p)	0.8857(2)	−0.0515(5)	−0.0075(4)	0.078(4)
O(8p)	0.8695(2)	−0.1018(3)	0.0396(4)	0.103(4)
N(1)	0.8905(2)	0.0439(3)	0.0124(3)	0.071(3)
C(1a)	0.8646(2)	0.0802(3)	0.0808(3)	0.055(3)
C(1′)	0.8171(2)	0.1188(3)	0.0501(3)	0.043(3)
O(1′)	0.8068(1)	0.1108(2)	−0.0217(2)	0.062(2)
O(1″)	0.7917(1)	0.1556(2)	0.1031(2)	0.053(2)
C(1b)	0.8909(2)	0.1384(4)	0.1366(4)	0.071(4)
O(1b)	0.8964(2)	0.2231(2)	0.1039(3)	0.078(3)
C(1g)	0.9423(3)	0.1046(6)	0.1606(6)	0.114(6)
C(1d1)	0.9676(3)	0.1625(6)	0.2082(7)	0.135(8)
C(1d2)	0.9310(3)	0.0130(5)	0.2033(7)	0.127(7)
Solvate				
O(1m)	0.3434(3)	0.2882(4)	0.6256(7)	0.236(9)
C(1m)	0.3487(3)	0.2194(5)	0.7015(5)	0.114(6)

Table 4. Final Atomic Coordinates of Complex III and Equivalent Values of the Isotropic Temperature Factors with Their esds in Parentheses

Atom	x	y	z	$U_{eq}/Å^2$
Pair I				
Brucine				
N(1)	−0.2000(2)	0.7807(1)	0.7878(4)	0.037(2)
C(2)	−0.1179(2)	0.8064(2)	0.7819(6)	0.038(3)
C(3)	0.0278(3)	0.7754(2)	0.9033(6)	0.047(3)
N(4)	0.0853(2)	0.7989(2)	0.7767(6)	0.052(3)
C(5)	0.0445(3)	0.7924(2)	0.5966(6)	0.050(3)
C(6)	−0.0205(3)	0.7529(2)	0.6095(6)	0.049(3)
C(7)	−0.0530(3)	0.7632(2)	0.7910(6)	0.040(3)
C(8)	−0.1041(2)	0.7199(2)	0.8481(6)	0.044(3)
C(9)	−0.0750(3)	0.6734(2)	0.9042(6)	0.045(3)
C(10)	−0.1327(3)	0.6379(2)	0.9390(7)	0.047(3)
C(11)	−0.2191(3)	0.6487(2)	0.9180(6)	0.042(3)
C(12)	−0.2468(2)	0.6952(2)	0.8674(6)	0.041(3)
C(13)	−0.1861(2)	0.7311(2)	0.8361(5)	0.037(3)
C(14)	0.0190(3)	0.8078(2)	1.0602(7)	0.056(3)
C(15)	−0.0237(3)	0.8562(2)	0.9942(6)	0.049(3)
C(16)	−0.1135(2)	0.8427(2)	0.9322(6)	0.042(3)
C(17)	−0.1736(3)	0.8845(2)	0.8833(6)	0.046(3)
C(18)	−0.0743(3)	0.9467(2)	0.8160(8)	0.056(4)
C(19)	0.0039(3)	0.9201(2)	0.7752(7)	0.055(4)
C(20)	0.0258(3)	0.8780(2)	0.8566(7)	0.050(3)
C(21)	0.1066(3)	0.8516(2)	0.8228(7)	0.055(3)
C(22)	−0.2685(3)	0.8078(2)	0.8183(5)	0.040(3)
C(23)	−0.2560(3)	0.8631(2)	0.8038(6)	0.044(3)
C(24)	−0.0271(3)	0.5792(2)	1.0313(8)	0.069(4)
C(25)	−0.3580(3)	0.6185(2)	0.9151(9)	0.072(5)
O(1)	−0.1473(2)	0.9185(1)	0.7589(4)	0.053(2)
O(2)	−0.3344(2)	0.7897(1)	0.8473(4)	0.048(2)
O(3)	−0.1132(2)	0.5906(1)	0.9934(4)	0.053(2)
O(4)	−0.2693(2)	0.6101(1)	0.9509(5)	0.053(2)
Pht-*threo*-L-Hyleu				
C(1p)	0.2710(4)	0.5161(2)	1.1205(7)	0.057(3)
C(2p)	0.3368(4)	0.4902(2)	1.2080(7)	0.068(3)
C(3p)	0.4179(4)	0.5035(2)	1.1979(7)	0.063(3)
C(4p)	0.4379(3)	0.5447(2)	1.1059(7)	0.061(3)
C(5p)	0.3736(2)	0.5713(2)	1.0192(5)	0.039(2)
C(6p)	0.2923(3)	0.5568(2)	1.0279(5)	0.041(2)
C(7p)	0.2384(3)	0.5928(2)	0.9278(6)	0.043(2)
O(7p)	0.1631(2)	0.5920(1)	0.9065(4)	0.055(2)
C(8p)	0.3746(3)	0.6172(2)	0.9150(6)	0.043(2)
O(8p)	0.4319(2)	0.6421(1)	0.8810(5)	0.059(2)
N(1)	0.2908(2)	0.6274(1)	0.8621(5)	0.041(2)
C(1a)	0.2666(3)	0.6738(2)	0.7703(6)	0.040(2)
C(1′)	0.2408(3)	0.7127(2)	0.9007(6)	0.049(2)
O(1′)	0.2346(3)	0.7012(2)	1.0510(5)	0.081(2)
O(1″)	0.2284(2)	0.7549(1)	0.8349(5)	0.060(2)
C(1b)	0.2013(3)	0.6679(2)	0.6190(6)	0.050(3)
O(1b)	0.1192(2)	0.6654(1)	0.6828(5)	0.060(2)
C(1g)	0.2174(3)	0.6251(2)	0.5028(5)	0.047(2)
C(1d1)	0.1476(4)	0.6195(3)	0.3603(7)	0.068(3)
C(1d2)	0.3008(3)	0.6306(2)	0.4261(7)	0.061(3)

Table 4. (Continued)

Atom	x	y	z	$U_{eq}/Å^2$
Pair II				
Brucine				
N(1)	0.6885(2)	0.8296(1)	0.2599(4)	0.039(2)
C(2)	0.6055(2)	0.8053(2)	0.2557(5)	0.037(2)
C(3)	0.4678(2)	0.8437(2)	0.3500(6)	0.043(2)
N(4)	0.4016(2)	0.8147(2)	0.2389(5)	0.051(2)
C(5)	0.4286(3)	0.8117(2)	0.0555(7)	0.054(3)
C(6)	0.4973(3)	0.8496(2)	0.0503(6)	0.046(2)
C(7)	0.5415(3)	0.8480(2)	0.2359(5)	0.041(2)
C(8)	0.5944(2)	0.8929(2)	0.2761(5)	0.036(2)
C(9)	0.5695(3)	0.9418(2)	0.2990(6)	0.045(2)
C(10)	0.6299(3)	0.9783(2)	0.3286(6)	0.045(2)
C(11)	0.7155(3)	0.9649(2)	0.3321(6)	0.042(2)
C(12)	0.7401(3)	0.9172(2)	0.3086(6)	0.044(2)
C(13)	0.6782(3)	0.8813(2)	0.2796(5)	0.040(2)
C(14)	0.4865(3)	0.8187(2)	0.5228(6)	0.048(2)
C(15)	0.5241(3)	0.7670(2)	0.4927(6)	0.052(3)
C(16)	0.6095(3)	0.7764(2)	0.4250(6)	0.044(2)
C(17)	0.6664(3)	0.7324(2)	0.4060(6)	0.046(2)
C(18)	0.5626(3)	0.6684(2)	0.3634(8)	0.066(3)
C(19)	0.4817(3)	0.6945(2)	0.3090(7)	0.058(3)
C(20)	0.4647(3)	0.7388(2)	0.3659(7)	0.052(3)
C(21)	0.3840(3)	0.7641(2)	0.3114(7)	0.056(3)
C(22)	0.7580(2)	0.8038(2)	0.3088(5)	0.041(2)
C(23)	0.7441(3)	0.7483(2)	0.3200(6)	0.049(2)
C(24)	0.5279(3)	1.0403(2)	0.3598(8)	0.060(3)
C(25)	0.8549(3)	0.9923(2)	0.3537(9)	0.073(3)
O(1)	0.6322(2)	0.6934(1)	0.2971(5)	0.056(2)
O(2)	0.8270(2)	0.8224(1)	0.3364(4)	0.051(2)
O(3)	0.6130(2)	1.0266(1)	0.3565(4)	0.053(2)
O(4)	0.7689(2)	1.0034(1)	0.3627(5)	0.058(2)
Pht-*threo*-L-Hyleu				
C(1p)	0.2355(4)	1.0930(2)	0.5309(7)	0.062(3)
C(2p)	0.1767(5)	1.1243(2)	0.5926(9)	0.078(4)
C(3p)	0.0904(5)	1.1161(2)	0.5503(9)	0.082(4)
C(4p)	0.0634(3)	1.0767(2)	0.4482(8)	0.070(3)
C(5p)	0.1256(3)	1.0445(2)	0.3927(7)	0.050(2)
C(6p)	0.2079(3)	1.0539(2)	0.4344(6)	0.047(2)
C(7p)	0.2563(3)	1.0139(2)	0.3562(6)	0.045(2)
O(7p)	0.3303(2)	1.0094(2)	0.3640(5)	0.062(2)
C(8p)	0.1171(3)	0.9988(2)	0.2893(6)	0.047(2)
O(8p)	0.0551(2)	0.9781(2)	0.2307(5)	0.065(2)
N(1)	0.1982(2)	0.9832(1)	0.2680(5)	0.042(2)
C(1a)	0.2134(3)	0.9362(2)	0.1813(5)	0.039(2)
C(1′)	0.2276(3)	0.8934(2)	0.3132(6)	0.048(2)
O(1′)	0.2175(3)	0.9016(2)	0.4658(5)	0.081(3)
O(1″)	0.2456(2)	0.8528(1)	0.2463(5)	0.055(2)
C(1b)	0.2843(2)	0.9382(2)	0.0586(6)	0.042(2)
O(1b)	0.3634 (2)	0.9344(1)	0.1566(5)	0.064(2)
C(1g)	0.2808(3)	0.9827(2)	−0.0613(6)	0.049(2)
C(1d1)	0.3511(4)	0.9802(3)	−0.1809(8)	0.076(4)
C(1d2)	0.1974(3)	0.9859(2)	−0.1683(7)	0.059(3)
Solvate				
O(1w)	0.1758(2)	0.7600(1)	0.3096(4)	0.060(2)
O(2w)	0.3082(2)	0.8361(2)	0.6934(6)	0.082(3)

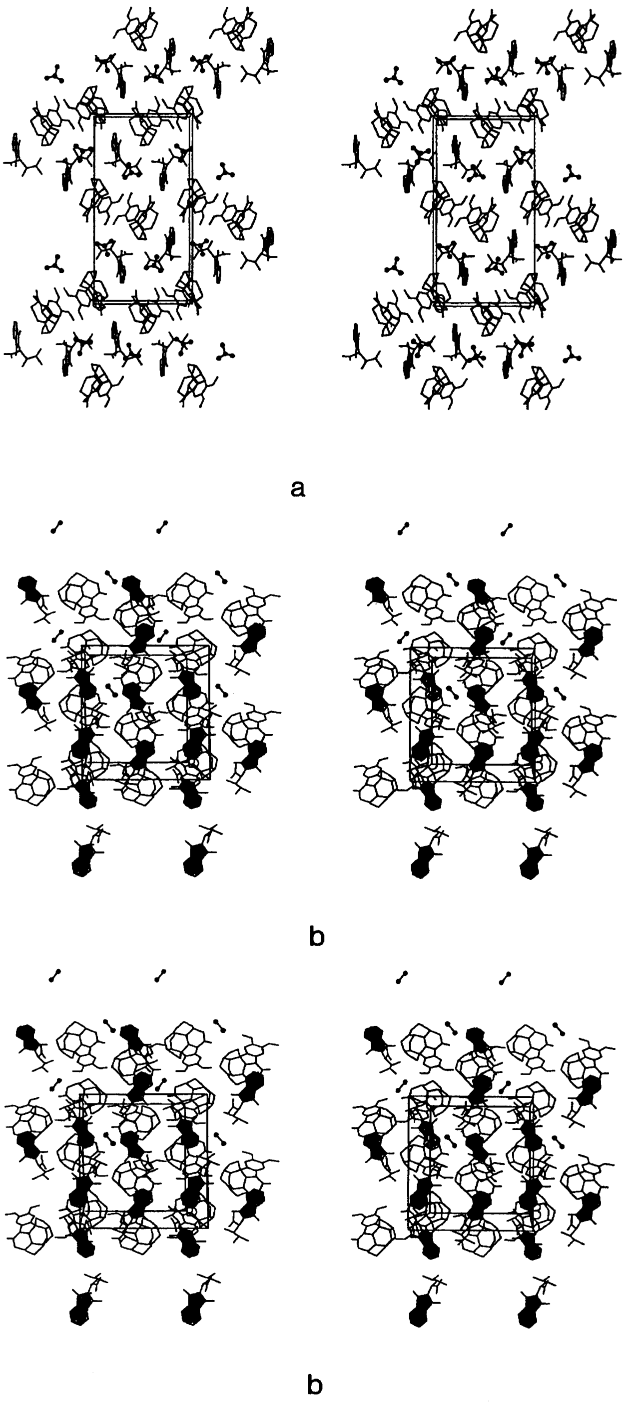

Fig. 3. Stereoscopic views of crystal packings of Complexes I (a, *c*-projection), II (b, *a*-projection), and III (c, *c*-projection). For the sake of clarity, figure (b) is shown only in the range of $0 \leq a \leq 1/2$, i.e., half of total molecular packing in the crystal lattice concerning the *a*-axis.

Table 5. Hydrogen Bonds and Short Contacts (Less Than 3.5 Å)

at x, y, z,	at	Symmetry operation	Distance/Å
Complex I			
BC	PL		
C(18)	O(7p)	$x-1/2,3/2-y,1-z$	3.334(8)
C(19)	O(7p)	$x-1/2,3/2-y,1-z$	3.235(7)
C(3)	O(1″)	x,y,z	3.301(6)
N(4)	C(1′)	x,y,z	3.190(6)
N(4)	O(1′)	x,y,z	3.095(6)
N(4)	O(1″)	x,y,z	2.687(6)
C(5)	O(1′)	x,y,z	3.111(7)
C(6)	O(1′)	x,y,z	3.438(7)
C(9)	O(1b)	x,y,z	3.490(6)
C(21)	O(1″)	x,y,z	3.384(7)
C(24)	O(1b)	x,y,z	3.452(7)
O(2)	C(2p)	$1-x,y+1/2,5/2-z$	3.432(8)
O(2)	C(3p)	$1-x,y+1/2,5/2-z$	3.227(8)
C(25)	O(1b)	$3/2-x,2-y,z+1/2$	3.257(7)
PL	PL		
O(1″)	C(4p)	$x,y,z-1$	3.445(7)
C(1g)	O(1′)	$x+1/2,3/2-y,2-z$	3.375(6)
C(1d1)	O(8p)	$x+1/2,3/2-y,2-z$	3.493(6)
C(1d1)	O(1′)	$x+1/2,3/2-y,2-z$	3.215(7)
C(1d2)	O(1′)	$x+1/2,3/2-y,2-z$	3.295(7)
Solvent	PL		
C(1et)	C(4p)	x,y,z	3.332(9)
O(1et)	O(1″)	$x,y,z+1$	2.85(2)
Complex II			
BC	PL		
O(3)A[a]	C(3p)A	$1-x,y+1/2,1/2-z$	3.41(1)
N(1)A	O(1″)B	$x,y+1,z$	3.267(5)
C(2)A	O(1″)B	$x,y+1,z$	3.386(5)
C(5)A	O(8p)B	$x,y+1,z$	3.169(7)
C(22)A	O(1″)B	$x,y+1,z$	3.483(6)
C(3)A	C(1′)A	x,y,z	3.484(7)
C(3)A	O(1″)A	x,y,z	3.187(5)
N(4)A	C(1′)A	x,y,z	3.221(6)
N(4)A	O(1′)A	x,y,z	3.293(5)
N(4)A	O(1″)A	x,y,z	2.666(5)
C(21)A	O(1′)A	x,y,z	3.200(6)
C(21)A	O(1″)A	x,y,z	3.470(6)
O(2)A	C(3p)B	$3/2-x,1-y,z+1/2$	3.41(2)
C(15)A	O(1′)B	$3/2-x,1-y,z+1/2$	3.404(6)
C(3)B	C(1′)B	x,y,z	3.457(6)
C(3)B	O(1″)B	x,y,z	3.185(5)
C(3)B	O(1b)B	x,y,z	3.488(6)
N(4)B	C(1′)B	x,y,z	3.179(6)
N(4)B	O(1′)B	x,y,z	3.215(5)
N(4)B	O(1″)B	x,y,z	2.627(5)
C(21)B	O(1′)B	x,y,z	3.201(6)
C(21)B	O(1″)B	x,y,z	3.497(6)
C(15)B	O(1′)A	$3/2-x,1-y,z-1/2$	3.484(6)
N(1)B	O(1″)A	x,y,z	3.379(5)
C(5)B	O(8p)A	x,y,z	3.030(7)
C(22)B	O(1″)A	x,y,z	3.346(6)
BC	BC		
O(2)A	C(5)A	$x,y+1,z$	3.434(7)
C(5)A	O(2)A	x,y,z	3.304(6)
Solvent	PL		
O(1m)	O(1″)A	$1-x,y-1/2,1/2-z$	3.382(9)
Solvent	BC		
O(1m)	O(1)B	$x-1/2,3/2-y,1-z$	3.44(1)
Complex III			
BC	PL		
C(3)A	O(1″)A	x,y,z	3.367(6)
N(4)A	O(1″)A	x,y,z	2.606(5)
C(6)A	O(1b)A	x,y,z	3.291(6)
C(21)A	O(1″)A	x,y,z	3.272(6)
C(24)A	O(7p)A	x,y,z	3.308(7)
C(24)A	O(8p)B	$-x,y-1/2,1-z$	3.419(7)
O(3)A	C(5p)B	$-x,y-1/2,1-z$	3.234(6)
O(3)A	C(8p)B	$-x,y-1/2,1-z$	3.312(6)
O(3)A	C(1d2)B	$-x,y-1/2,1-z$	3.467(6)
O(1)A	C(1p)A	$-x,y+1/2,2-z$	3.485(6)
C(21)B	O(1′)A	$x,y,z-1$	3.466(7)
C(3)B	O(1b)B	x,y,z	3.275(6)
N(4)B	O(1″)B	x,y,z	2.726(5)
N(4)B	O(1b)B	x,y,z	3.353(5)
C(6)B	O(1b)B	x,y,z	3.304(6)
C(9)B	O(1b)B	x,y,z	3.426(6)
C(21)B	O(1″)B	x,y,z	3.294(6)
C(24)B	O(7p)B	x,y,z	3.300(6)
C(25)B	O(8p)B	$x+1,y,z$	3.461(7)
C(24)B	C(8p)A	$1-x,y+1/2,1-z$	3.448(7)
C(24)B	O(8p)A	$1-x,y+1/2,1-z$	3.422(6)
C(25)B	O(7p)A	$1-x,y+1/2,1-z$	3.370(7)
O(3)B	C(5p)A	$1-x,y+1/2,1-z$	3.177(5)
O(3)B	C(8p)A	$1-x,y+1/2,1-z$	3.251(5)
O(4)B	C(6p)A	$1-x,y+1/2,1-z$	3.429(5)
O(4)B	C(7p)A	$1-x,y+1/2,1-z$	3.304(6)
O(4)B	O(7p)A	$1-x,y+1/2,1-z$	3.420(5)
O(4)B	C(1g)A	$1-x,y+1/2,1-z$	3.462(6)
BC	BC		
O(2)A	C(15)B	$x-1,y,z$	3.486(6)
O(2)A	C(16)B	$x-1,y,z$	3.346(5)
C(16)A	O(2)B	$x-1,y,z+1$	3.393(5)
O(2)A	C(2)B	$x-1,y,z+1$	3.410(5)
O(2)A	N(1)B	$x-1,y,z+1$	3.369(5)
Solvent	BC		
O(1w)	C(14)A	$x,y,z-1$	3.322(6)
O(2w)	C(5)B	$x,y,z+1$	3.349(7)
O(1w)	C(5)A	x,y,z	3.310(6)
O(1w)	C(21)B	x,y,z	3.361(6)
O(2w)	C(14)B	x,y,z	3.293(6)
Solvent	PL		
O(1w)	O(1′)A	$x,y,z-1$	2.786(6)
O(1w)	C(1b)A	x,y,z	3.462(6)
O(1w)	O(1″)B	x,y,z	2.816(5)
O(2w)	O(1″)A	x,y,z	2.816(6)
O(2w)	C(1′)B	x,y,z	3.490(6)
O(2w)	O(1′)B	x,y,z	2.828(6)

[a] The suffix letters A and B represent two crystallographically-independent molecules.

Several kinds of interactions could be observed between the BC and PL molecules. Among them, the most significant interactions are shown in Fig. 4. A commonly observed interaction is that the protonated N(4) atom of BC is hydrogen-bonded to the deprotonated carboxyl oxygen of PL, and consequently van der Waals short contacts including electrostatic interactions are formed between these regions, where the β-hydroxyl group of

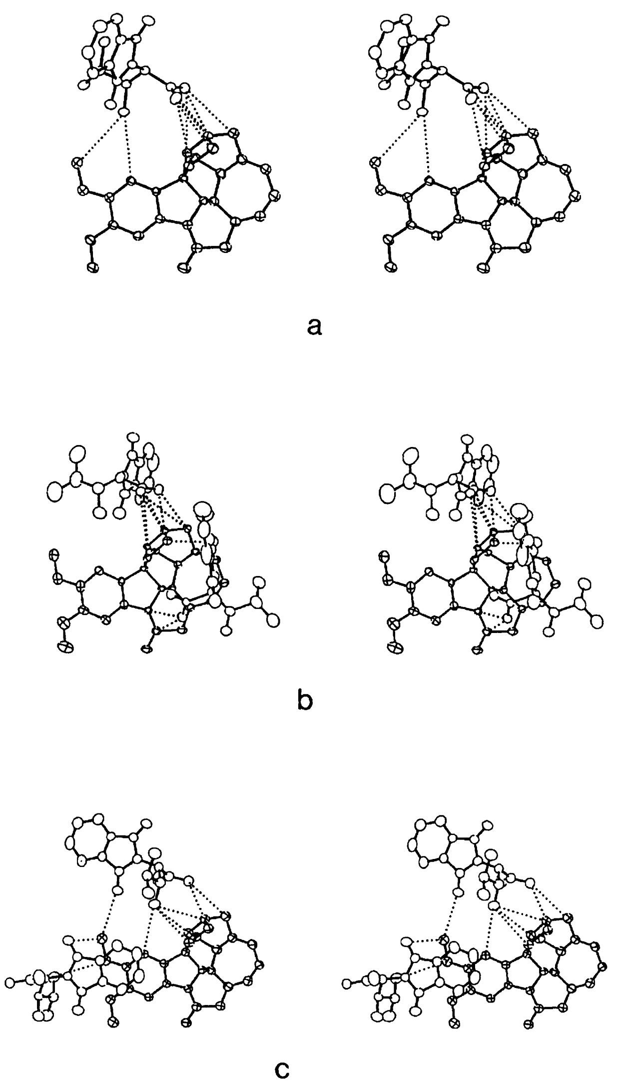

Fig. 4. Stereoscopic views of characteristic interaction modes formed between BC and PL molecules in Complexes I (a), II (b), and III (c). Interatomic short contacts are shown by dotted lines. Figures (b) and (c) show the interaction modes of BC molecule A (ellipsoidal circles) with two independent PL molecules, respectively. Almost the same interactions were also observed concerning BC molecule B.

PL also plays an important role in the electrostatic short contacts with the BC C(3), N(4), C(6), C(9), or C(24) atoms. Since this binding mode is common for all complex crystals, we call this interaction site the 'interfacial interaction' site of BC for the binding with a PL molecule, which consists of the upper side of the BC molecule shown in Fig. 4, i.e., the piperidine ring and the upper part of the methoxyindole ring moiety.

Short-contact interactions between one of the two methoxyl groups [the C(24) and O(3) atoms] of BC and the Leu side-chain methyl group of PL appear to be important for molecular binding in Complex II, because a significant nuclear Overhauser effect (NOE) was measured in the chloroform solution of Complex II, but not of Complex I.[11)]

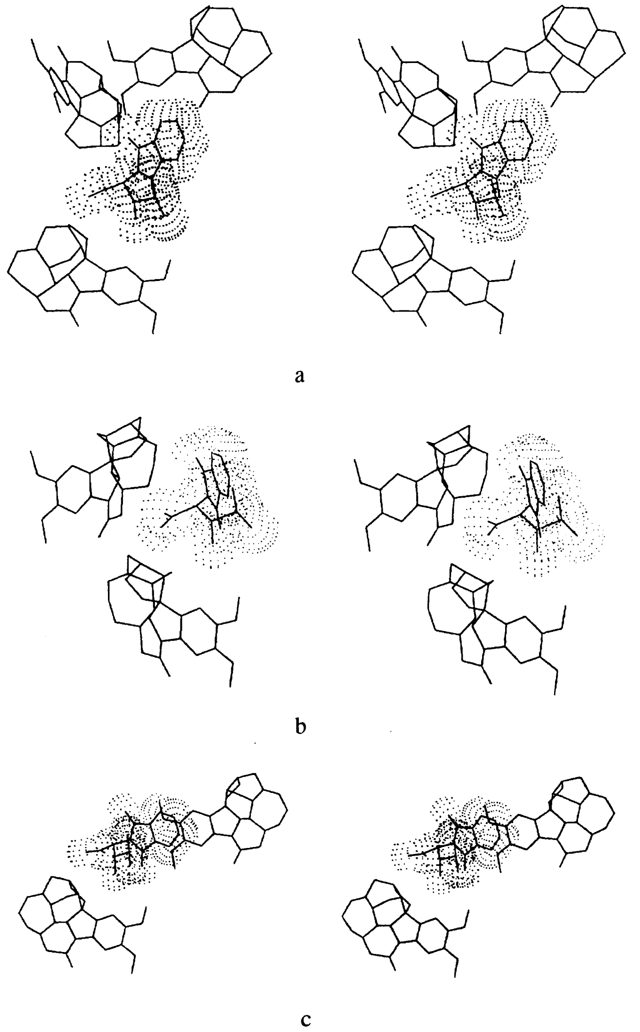

Fig. 5. Stereoscopic views of BC molecular arrangements formed in Complexes I (a), II (b), and III (c) for chiral recognition of a PL molecule (dot surface). In order to lock the PL D-isomer at (x, y, z), three BC molecules are spatially arranged in (a), where these BC molecules are related to one another by the symmetry operations of $(1-x,\ y-1/2,\ 5/2-z)$ and $(x+1/2,\ 3/2-y,\ 1-z)$. Two crystallographically-independent BC molecules of molecule A at (x, y, z) and molecule B at (x, y, z) in (b) and of molecule A at (x, y, z) and molecule B at $(1-x,\ y-1/2,\ 1-z)$ in (c) are arranged so as to selectively lock the PL L-isomer (molecule A at (x, y, z)) in (b) and (c). Nearly the same situations were also formed for the recognition of PL molecule B in Complexes II and III.

In addition to the above-mentioned interfacial interaction between both molecules, other notable interaction modes are formed in the complex crystals with the L-isomer. In Complex II, significant ionic interactions are formed between the BC N(1) and PL carboxyl oxygen moieties [Fig. 4b], where the carboxyl group is lo-

Table 6. Selected Torsion Angles of BC and PL Molecules

	Complex I	Complex II		Complex III	
		Mol-A	Mol-B	Mol-A	Mol-B
BC					
C(2)-N(1)-C(13)-C(8)	−6.4(4)	−5.4(3)	−4.3(3)	−0.5(4)	−1.2(4)
C(2)-N(1)-C(22)-C(23)	7.2(5)	12.7(3)	11.9(3)	10.0(4)	5.1(4)
C(16)-C(17)-C(23)-C(22)	3.3(5)	10.8(4)	12.9(4)	7.3(5)	5.6(5)
O(1)-C(17)-C(23)-C(22)	126.9(6)	135.9(4)	137.0(4)	131.2(5)	125.8(5)
N(1)-C(22)-C(23)-C(17)	−32.8(5)	−42.2(4)	−43.4(4)	−36.9(5)	−31.7(4)
O(2)-C(22)-C(23)-C(7)	147.7(7)	140.6(4)	138.9(5)	148.9(6)	148.1(6)
C(9)-C(10)-O(3)-C(24)	−3.8(5)	5.9(4)	1.6(4)	7.8(6)	20.0(5)
C(12)-C(11)-O(4)-C(25)	−8.3(5)	5.3(4)	5.6(4)	11.3(9)	11.4(5)
PL					
C(7p)-N(1)-C(1a)-C(1′)	99.5(4)	77.4(4)	75.4(4)	67.6(5)	68.3(5)
N(1)-C(1a)-C(1′)-O(1′)	15.1(4)	6.4(4)	−7.3(5)	3.4(5)	9.0(5)
N(1)-C(1a)-C(1′)-O(1″)	−167.9(5)	−176.2(4)	172.5(4)	−177.4(5)	−173.9(5)
N(1)-C(1a)-C(1b)-C(1g)	50.3(4)	−46.2(4)	−45.0(4)	−44.0(5)	−46.8(6)
N(1)-C(1a)-C(1b)-O(1b)	−78.5(4)	80.2(3)	81.0(4)	78.3(5)	79.9(6)
C(1a)-C(1b)-C(1g)-C(1d1)	56.9(4)	−177.9(5)	176.8(4)	175.8(8)	176(1)
C(1a)-C(1b)-C(1g)-C(1d2)	178.6(5)	−55.8(4)	−59.6(4)	−59.6(5)	−50.8(8)

cated on the indole plane of BC. Alternately, two BC methoxyl groups in Complex III play a role in stacking formation with the phthaloyl ring of a neighboring PL [Fig. 4c], where the dihedral angle of both rings and the averaged spacing are 18.4 ° and 3.52 Å for BC molecule A–PL molecule B and 27.0° and 3.63 Å for BC molecule B—PL molecule A.

D/L Recognition. It is reasonable to consider that the chiral recognition of a guest molecule by BC is largely dependent on the BC molecular arrangement in the crystal structure, in addition to direct and specific interactions with the guest molecule. The minimal molecular arrangements of BC in the present complex crystals, which would be necessary to recognize the D/L chirality of a PL molecule, are shown in Fig. 5, where the van der Waals sphere of the PL molecule is shown by a dot surface.

In Complex I, three BC molecules, which are related to one another by 2-fold screw symmetry, form a receptor surface suitable for the binding of the D-isomer of PL (Fig. 5a). Spatial dispositions of these BC molecules tightly lock the D-isomer by van der Waals, electrostatic, and hydrogen-bond interactions. On the other hand, the recognition of the PL L-isomer in both Complexes II and III is achieved by the cooperation of two independent BC molecules, although their recognition modes are rather different from each other (Figs. 5b and 5c). In Complex II, two independent BC molecules are arranged in such a way that one of them is linked with PL through the interfacial interaction and the other through the N···O=C ionic interaction. In this molecular arrangement of BC, the orientation of the PL phthaloyl group is severely restricted in the direction of the L-configuration. On the other hand, Complex III forms another type of BC molecular arrangement to recognize the PL L-isomer. The binding pocket created by two independent BC molecules is specific for the L-isomer, in which the PL molecule is tightly locked by interfacial and aromatic stacking interactions. The binding of the D-isomer to such a pocket is not allowed because of the steric hindrance between the Leu side chain and the BC molecule.

The present insights provide an explanation for how the BC molecule recognizes or classifies the PL D/L-isomer in the crystalline state. The present crystal structures indicate that BC requires two crystallographically independent molecules for the recognition of the L-isomer, while the recognition for the D-isomer is achieved by only one molecule. The corrugated monolayer sheet structure of the BC molecules observed in Complex I, a molecular arrangement of BC most frequently observed for the optical resolution of either of the optical isomers of guest molecules,[2) could be the most suitable environment for the selective interaction with the D-isomer, but not the L-isomer. For the recognition of the L-isomer, thus, it could be thought that another type of molecular arrangement is required, and consequently, two crystallographically independent BC molecules are used to achieve this end. Thus, it may be said that the recognition of the L-isomer by BC molecules requires a more elaborate shape concerning the acceptor surface (or pocket) than that for the D-isomer.

It was made clear by the present study that the crystal structure (or molecular arrangement) of brucine complexed with an N-protected amino acid is quite different between the D- and L-isomers, and this is a reason why either of the D/L isomers is selectively precipitated out in the coexistence with brucine molecules.

References

1) J. Jacques, A. Collet, and S. H. Wilan, "Enantiomers,

Racemates and Resolutions," Wiley, New York (1981), p. 215.

2) R. O. Gould and M. D. Walkinshaw, *J. Am. Chem. Soc.*, **106**, 7840 (1984).

3) R. O. Gould, P. Taylor, and M. D. Walkinshaw, *Acta Crystallogr., Sect. A*, **40**, C86 (1984); F. Toda, K. Tanaka, and H. Ueda, *Tetrahedron Lett.*, **22**, 4669 (1981); G. Quinkert, H. -G. Schmalz, E. M. Dzierzynski, G. Durner, and J. W. Bats, *Angew. Chem., Int. Ed. Engl.*, **25**, 992 (1986).

4) J. G. Stroh, K. L. Rinehart, Jr., J. C. Cook, T. Kihara, M. Suzuki, and T. Arai, *J. Am. Chem. Soc.*, **108**, 858 (1986); C. Rossi, T. Tuttobello, M. Ricci, C. G. Casinovi, and L. Radics, *J. Antibiot.*, **40**, 130 (1987).

5) S. Kuwata, J. Tanaka, Y. Sakamoto, N. Onda, T. Yamada, and T. Miyazawa, *Chem. Lett.*, **1989**, 2031.

6) G. M. Sheldrick, "Crystallographic Computing 3," Oxford University Press, Oxford (1985), p. 175.

7) E. Egert and G. M. Sheldrick, *Acta Crystallogr., Sect. A*, **41**, 262 (1985).

8) G. M. Sheldrick, "SHELX-76. Program for Crystal Structure Determination," University of Cambridge, England (1976).

9) The tables of the anisotropic temperature factors of non-H atoms, atomic coordinates and isotropic thermal parameters of H atoms, bond lengths, bond angles, torsion angles, and the observed and calculated structure factors are kept as Document No. 66011 at the Office of the Editor of the Bull. Chem. Soc. Jpn.

10) S. S. B. Glover, R. O. Gould, and M. D. Walkinshaw, *Acta Crystallogr., Sect. C*, **41**, 990 (1985).

11) S. Kuwata, N. Onda, T. Yamada, T. Miyazawa, and M. Sugiura, "The 59th Annual Meeting of the Chemical Society of Japan," Kanagawa, Japan, April 1990, Abstr., No. 3C512.